XVIII. ULUSAL MEKANİK KONGRESİ
26 - 30 Ağustos 2013, Celal Bayar Üniversitesi, Manisa

AN INTEGRAL EQUATION APPROACH FOR THE SOLUTION OF THE STOKES FLOW WITH HERMITE SURFACES

Kayhan Ata, Süleyman Karaca and Mehmet Sahin[1]
Faculty of Aeronautics and Astronautics, Istanbul Technical University, Maslak, Istanbul, 34

ABSTRACT

An integral equation method has been developed to solve the three-dimensional Stokes flow using a quadrilateral Hermite based function approach to the boundary integral method. The numerical solutions are obtained by utilizing the boundary collocation method as well as the continuous distribution of Stokeslets, which are the fundamental solutions of the steady Stokes equations. The quadrilateral surface elements are based on the bi-cubic hermite functions that allows the continuous variation of the surface normal vectors between neighboring elements. The singular integrations are evaluated numerically using the *tanh-sinh* quadrature rule meanwhile non-singular integrals are evaluated using the Gauss-Legendre quadrature rule. The numerical algorithm is initially validated for the three-dimensional unbounded Stokes flow around a sphere. Then the algorithm is applied to the sedimentation of spherical particles.

Keywords: Integral equation method, Stokes flow, Hermite functions, singular integrals, sedimentation.

ÖZET

Üç boyutlu Stokes akışını çözmek amacıyla sınır integral yöntemiyle beraber dörtgen Hermit yüzeyler kullanılarak bir integral denklem yöntemi geliştirilmiştir. Sayısal sonuçlar, sınır sıralama yönteminden ve daimi Stokes denkleminin temel çözümleri olan Stokesletlerin sürekli dağılımından yararlanılarak elde edilmiştir. Dörtgen yüzey elemanları, komşu elemanlar arasındaki yüzey normal vektörünün sürekliliğini sağlayan hermite fonksiyonları kullanılarak tanımlanmıştır. Tekil integraller *tanh-sinh* tümlev yöntemi, tekil olmayan integraller ise Gauss-Legendre yöntemi kullanılarak sayısal olarak hesaplanmıştır. Sayısal algoritma ilk olarak küre etrafindaki üç boyutlu Stokes akışında doğrulanmıştır. Sonrasında algoritma küresel parçacıkların sedimantasyonu problemi için uygulanmıştır.

[1] E-mail: msahin.ae00@gtalumni.org

Anahtar kelimeler: İntegral denklem yöntemi, Stokes akışı, Hermite fonksiyonları, tekil integraller, sedimantasyon.

1 INTRODUCTION

Over the past decades, the boundary integral methods have emerged to be a very powerful technique for studying the flow behavior at vanishingly small Reynolds numbers, i.e. under Stokes flow conditions. The application of the present method to the three-dimensional Stokes flow was first formulated by Youngren and Acrivos [1] for an unbounded fluid past a single solid particle as a distribution of Stokeslets over the particle surface. Then the method was quickly adopted for several other flow problems at very low Reynolds numbers including the flow past deformable drops and bubbles [2], the flows of suspensions of rigid particles [3], the microscopic flow in porous media [4], the deformation of red blood cells [5], the swimming of microscopic organisms [6], etc. The main advantages of the boundary integral equation method is that it reduces the solution of full three-dimensional fluid flow problem into the two-dimensional problem of determining source distributions on the bounding surfaces, which does not require the construction of volume mesh. In addition, the far-field boundary conditions are satisfied exactly for exterior fluid flow problems. However, the numerical approach has also several disadvantages. The first one is that the numerical algorithm does lead to a dense system of algebraic equations and it is very difficult to implement efficiently on highly parallel machines. The second one is that the integral equation formulation leads to singular integrals which requires special treatment.

The exact integration of the singular functions can be calculated either analytically or by using special numerical techniques. The numerical integration techniques are mostly based on the variable mappings which cluster quadrature points close to the position of the singularity. Muldowney and Higdon [7] showed that the transformed quadrature methods for singular and nearly singular integrals can be constructed for the requirements of the spectral element. Chan et al. [8] proposed an adaptive subdomain integration scheme that dramatically improved the integration accuracy and provided convergent solutions for problems of very small gaps. Duffy [9] suggested the transformation of integration over a triangular surface having a singular vertex into an integration over a unit square. The transformation cancels the singularity. However, this approach is accurate only for sufficiently regular triangles. In addition, there is another type of approach which replaces singular kernel by a regularized kernel [10]. Another approach is to employ the *tanh-sinh* quadrature rule proposed by Takahasi and Mori [11]. As far as the author knowledge goes, the *tanh-sinh* quadrature rule is not employed for the integral equation formulation of the Stokes flow. This approach uses change of variables to transform an integral on the interval [-1,1] to an integral between [-∞,∞]. After the transformation, the integrand decays with a double exponential rate. Although *tanh-sinh* quadrature is less efficient than Gaussian quadrature for smooth integrands, but unlike Gaussian quadrature tends to work equally well with integrands having singularities or infinite derivatives at one or both endpoints of the integration interval.

Although the singular kernel could be evaluated using the transformed quadrature methods, the discontinuities in the normal vector around the collocation/singularity point may cause irregularities in the numerical solution. One possible approach to remedy the numerical solution is to employ more smooth variation of boundary surface. A cubic Hermite polynomial which yields smoothly blended surface elements can be employed over unstructured quadrilateral elements. The Hermite polynomial interpolation requires the function value and its derivatives at the vertices. Although the coordinate of vertices are known, the tangent values at vertices has to be computed. The tangent values can be calculated from the unique normal vector at vertices.

The purpose of the present work is to combine the bi-cubic Hermite polynomial with the *tanh-sinh* quadrature rule in order to develop a sufficiently robust Stokes solver based on the integral equation formulation. The numerical algorithm uses unstructured quadrilateral elements over the domain boundaries and the unknown function values are distributed over the vertices of quadrilateral elements. The singular integrations are evaluated numerically using the *tanh-sinh* quadrature rule meanwhile non-singular integrals are evaluated using the Gauss-Legendre quadrature rule. The numerical algorithm is initially validated for the three-dimensional unbounded Stokes flow around a sphere. Then the algorithm is applied to the sedimentation of spherical particles.

2 MATHEMATICAL AND NUMERICAL FORMULATION

2.1 The Stokes Flow Equation

Incompressible fluid flow problems where viscous forces are dominant, can be described by the divergence-free condition and the Stokes equation

$$\nabla \cdot \mathbf{u} = 0 \tag{1}$$

$$-\nabla P + \mu \nabla^2 \mathbf{u} + \rho \mathbf{g} = 0 \tag{2}$$

Here **u** is the fluid velocity, μ the viscosity of the fluid, **P** is the pressure and **g** is the body force.

2.2 The Boundary Integral Formulation

The fundamental solution to the Stokes equation **S**, called the Stokeslet, and its associated stress **T**, the Stokes-stresslet, are

$$S_{ik} = \frac{\delta_{ik}}{r} + \frac{\hat{\mathbf{x}}_i \hat{\mathbf{x}}_k}{r^3} \tag{3}$$

$$T_{ijk} = -6 \frac{\hat{\mathbf{x}}_i \hat{\mathbf{x}}_j \hat{\mathbf{x}}_k}{r^5} \tag{4}$$

where $\hat{\mathbf{x}} = \mathbf{x} - \mathbf{x_0}$ and $r = |\hat{\mathbf{x}}|$. The velocity at a point $\mathbf{x_0}$ on the boundary of the fluid domain S_B may be expressed in the integral form

$$\eta(\mathbf{x}_0)\mathbf{u}_k(\mathbf{x}_0) = -\frac{1}{4\pi\mu}\oiint_{S_B}[\mathrm{S}_{ik}\mathrm{t}_i(\mathbf{x}) - \mu\,\mathrm{T}_{ijk}\,u_i(\mathbf{x})\,\mathrm{n}_j]\mathrm{dS} \tag{5}$$

here

$$\eta(\mathbf{x}_0) = \begin{cases} 1/2, & \mathbf{x}_0 \in S_B \\ 1, & \mathbf{x_0} \in \Omega \end{cases} \tag{6}$$

In here, $\mathbf{t} = \sigma\,\mathbf{n}$ is traction vector and the normal vector $\mathbf{n}$ points into the fluid domain. For boundary value problems with velocity boundary conditions, the integral equation leads to Fredholm integral equations of the first kind

$$8\pi\mu u_k(\mathbf{x}_0) = \oiint_{S_B} t_i\left[\frac{\delta_{ik}}{r} + \frac{(\mathrm{x}_i - \mathrm{x}_{0_i})(\mathrm{x}_k - \mathrm{x}_{0_k})}{r^3}\right]dS \tag{7}$$

and the pressure field can be evaluated as follows:

$$8\pi P(\mathbf{x}_0) = \oiint_{S_B} t_i\left[2\frac{(\mathrm{x}_i - \mathrm{x}_{0_i})}{r^3}\right]dS \tag{8}$$

2.3 Quadrilateral Hermite Surfaces

Hermite interpolation problem requires a construction of a suitable planar curve fitting for a set of data, which consists of 4 vertex points, 8 tangent vectors and 4 second derivative vectors. The mixed second partial derivative vectors are often called the twist, because large values can cause a corkscrew-like twist at the corners. In here, the twist values are set to zero, which corresponds to a Ferguson surface. The parametric bi-cubic hermite surface is given by

$$r(u,v) = \begin{bmatrix} H_0(u) & H_1(u) & H_2(u) & H_3(u) \end{bmatrix}[G]\begin{bmatrix} H_o(v) \\ H_1(v) \\ H_2(v) \\ H_3(v) \end{bmatrix}, \quad u,v \in [0,1] \tag{9}$$

Where;

$$[G] = \begin{bmatrix} r(0,0) & r(0,1) & r_v(0,0) & r_v(0,1) \\ r(1,0) & r(1,1) & r_v(1,0) & r_v(1,1) \\ r_u(0,0) & r_u(0,1) & r_{uv}(0,0) & r_{uv}(0,1) \\ r_u(1,0) & r_u(1,1) & r_{uv}(1,0) & r_{uv}(1,1) \end{bmatrix} \tag{10}$$

and

$$H_0(u) = 1 - 3u^2 + 2u^3 \tag{11}$$

$$H_1(u) = 3u^2 - 2u^3 \tag{12}$$

$$H_2(u) = u - 2u^2 + u^3 \tag{13}$$

$$H_3(u) = u^3 - u^2 \tag{14}$$

are the Hermite polynomials. In here, the tangent vectors at vertices are calculated from unique normal vectors at vertices. In order to obtain the normal vectors, we employed the Mean Weighted by Sine and Edge Length Reciprocal (MWSELR) proposed by Max [12]. The six vertex normal calculation algorithms are compared with each other in [13] and the MWSELR algorithm turns out to be the best approach. In this approach, the normal vector is given by

$$\mathbf{n} = \sum_{i=1}^{n} \frac{\mathbf{n}_i \sin\alpha_i}{|E_i||E_{i+1}|} \tag{15}$$

where α_i is the angle between the two edge vectors $\mathbf{E}_i$ and $\mathbf{E}_{i+1}$ of the ith facet sharing the vertex.

2.4 Numerical Integration

The integral equation formulation requires the evaluation of integrals in the following form:

$$\int_{-1}^{1}\int_{-1}^{1} f(\xi,\eta)\det J d\xi d\eta \tag{16}$$

where the Jacobian of the transformation is given by

$$\det J = \left| \begin{Bmatrix} \dfrac{\partial x}{\partial \xi} \\ \dfrac{\partial y}{\partial \xi} \\ \dfrac{\partial z}{\partial \xi} \end{Bmatrix} + \begin{Bmatrix} \dfrac{\partial x}{\partial \eta} \\ \dfrac{\partial y}{\partial \eta} \\ \dfrac{\partial z}{\partial \eta} \end{Bmatrix} \right| \tag{17}$$

In here, the unknown traction vector components are represented using the bilinear interpolations over the quadrilateral elements.

$$\mathbf{t}(\xi,\eta)=\sum_{j=1}^{4} t_j N_j(\xi,\eta) \tag{18}$$

and the shape functions are given by

$$N_j(\xi,\eta)=\frac{(1+\xi\xi_j)(1+\eta\eta_j)}{4} \tag{19}$$

The numerical evaluation of the surface integrals is split into the singular and non-singular integrals. The non-singular integrals are evaluated using the Gauss-Legendre quadrature rule with N = 4. Meanwhile, the singular integrals are evaluated using the *tanh-sinh* quadrature rule. The quadrature points, x_j, and the weights, w_j, are computed to be:

$$x_j=\tanh\left(\frac{\pi}{2}\sinh jh\right) \tag{20}$$

$$w_j=\frac{\frac{\pi}{2}\cosh jh}{\cosh^2\left(\frac{\pi}{2}\sinh jh\right)} \tag{21}$$

where $h = 1/2^M$ with $M = 4$.

3 NUMERICAL RESULTS

In this section, the numerical algorithm is initially validated for the three-dimensional unbounded Stokes flow around a sphere. Then the algorithm is applied to the sedimentation of spherical particles.

3.1 Unbounded Stokes Flow around a Sphere

The first numerical test case corresponds to the unbounded steady Stokes flow around a sphere. The analytical solution for the velocity field past around a sphere with a radius R is given by

$$u_1(x_1,x_2,x_3)=\frac{3RU_1}{4}\left(\frac{1}{r^3}-\frac{R^2}{r^5}\right)x_1^2+\frac{RU_1}{4r}\left(3+\frac{R^2}{r^2}\right) \tag{22}$$

$$u_2(x_1,x_2,x_3)=\frac{3RU_1}{4}\left(\frac{1}{r^3}-\frac{R^2}{r^5}\right)x_2x_3 \tag{23}$$

$$u_3(x_1,x_2,x_3) = \frac{3RU_1}{4}\left(\frac{1}{r^3} - \frac{R^2}{r^5}\right)x_1x_3 \tag{24}$$

$$p(x_1,x_2,x_3) = p_0 - \frac{3\mu RU_1 x_1}{2r^3} \tag{25}$$

In here, r is the distance from the point **x** to the center of the sphere. Hydrodynamic traction vector on the sphere surface is given by

$$\mathbf{t} = \frac{3\mu}{2R}\mathbf{U} \tag{26}$$

Although the computed total drag is not good measure of solution accuracy, we will use it to validate our integral equation flow solver. For the present benchmark problem we employed three meshes: the coarse mesh with 1410 nodes and 1408 elements, the medium mesh with 2402 nodes and 2400 elements and the fine mesh 5402 nodes and 5400 elements. The computational quadrilateral surface mesh is shown in Figure 1 for the coarse mesh. The computed total drag values are tabulated in Table 3.1 and compared with the analytical exact value. The convergence analysis of the error indicates an algebraic convergence rate of O (Δh^3).

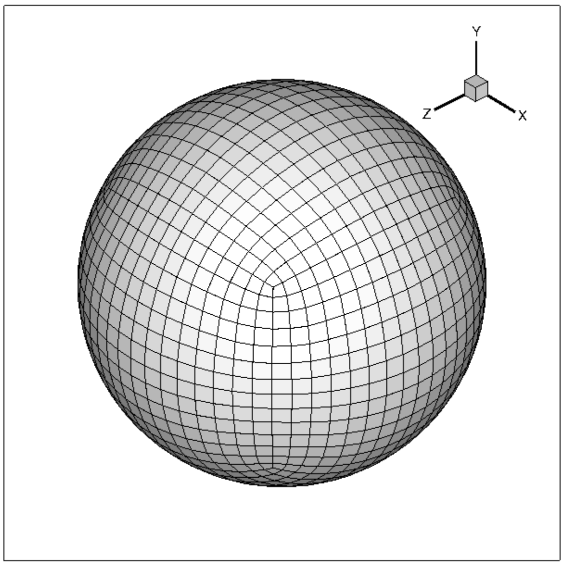

Figure 1: The computational coarse mesh with 2402 nodes and 2400 elements.

3.2 Sedimentation of Spherical Particles

In this section, initially a single sphere falling in an unbounded domain is numerically investigated. For the present problem, the radius of the sphere R is $1m$, the sphere density ρ is $0.4587 kg/m^3$ and gravitational acceleration g is $9.81 m/s^2$. The calculations are started from the rest with a time step of 0.005*s*. The time variation of the sphere free fall velocity is shown in Figure 2 and the sphere reaches the terminal velocity of 1*m/s* approximately after 0.8*s*.

Table 1: The convergence of the total drag for the Stokes flow past sphere.

Number of Elements	Total Drag (Numerical)	Exact Total Drag	Error
5400	18.849552908422041	18.849555921538	3.013116 e-06
2400	18.849545680592303	18.849555921538	1.024094 e-05
1408	18.849533161883699	18.849555921538	2.275965 e-05

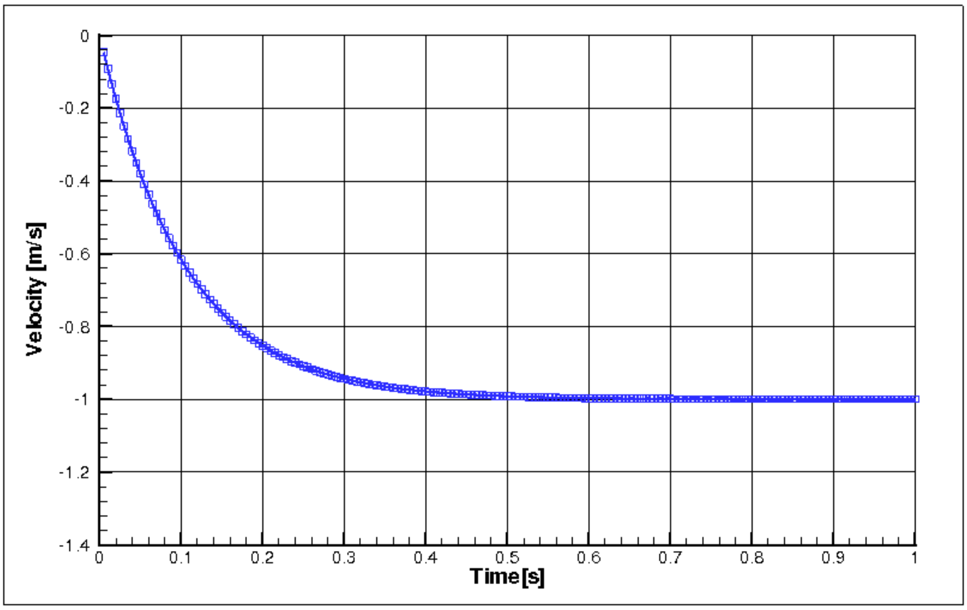

Figure 2: The time variation of the sphere velocity falling in an unbounded domain.

In the second case the trajectories of the multiple spheres are calculated. For the present case the same spheres are left for free fall starting from the rest. The spheres are 2.5*R* apart from each other. The computed final location of the spheres are shown in Figure 3. As the time evolves, the distance between the spheres are not changed significantly. The time variation of the sphere free fall velocity is shown in Figure 4 and the sphere reaches the terminal velocity higher than the single case.

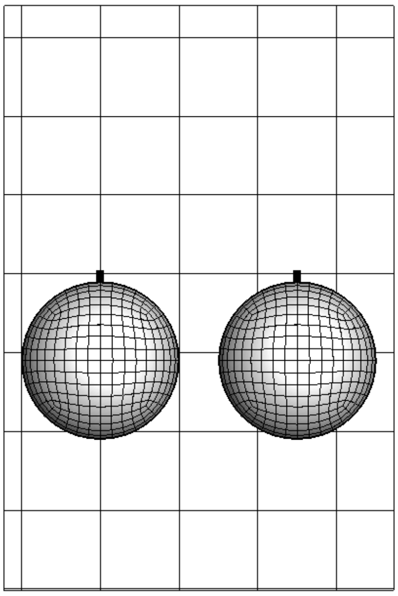

Figure 3: The computed locations of the spheres at $t = 1s$.

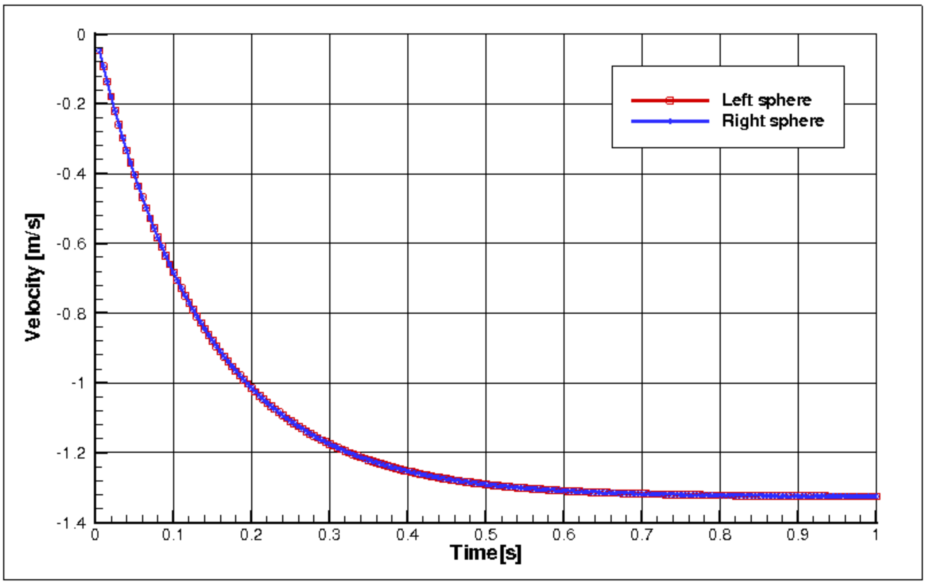

Figure 4: The time variation of the fall velocity for two spheres in an unbounded domain.

4 CONCLUSIONS

An integral equation method has been developed to solve the three-dimensional Stokes flow. The numerical algorithm based on the continuous representation of the surfaces with the parametric bi-cubic hermite polynomials combined with the *tanh-sinh* quadrature rule. The numerical algorithm is initially validated for the three-dimensional unbounded Stokes flow around a sphere. Then the algorithm is applied to the sedimentation of spherical particles. The numerical results indicate that the numerical method is sufficiently accurate for the Stokes fluid flow problems.

REFERENCES

[1] G. K. Youngren and A. Acrivos, Stokes flow past a particle of arbitrary shape: a numerical method of solution. *J. Fluid Mech*. 69, (1975) 377-403.

[2] G. K. Youngren and A. Acrivos, On the shape of a gas bubble in a viscous extensional flow. *J. Fluid Mech*. 76 (1976), 433-442.

[3] J. F. Brady, R. J. Phillips, J. C. Lester, and G. Bossis, Dynamic simulation of hydrodynamically interacting suspensions. *J. Fluid Mech*. 195 (1988), 257-280.

[4] R. E. Larson and J. J. L. Higdon, Microscopic flow near the surface of two-dimensional porous media. Part 1. Axial flow. *J. Fluid Mech*. 166 (1986), 449-472.

[5] C. Pozrikidis, The axisymmetric deformation of a red blood cell in a uniaxial straining Stokes flow. *J. Fluid Mech*. 216 (1990), 231-254.

[6] G. J. Hancock, The self-propulsion of microscopic organisms through liquids. *Proc. Roy. Soc. A* 217 (1953), 96-121.

[7] G. P. Muldowney and J. J. L. Higdon, A spectral boundary element approach to three-dimensional Stokes flow. *J. Fluid Mech*. 298 (1995), 167-192.

[8] C. Y. Chan, A. N. Beris and S. G. Advani, Second-order boundary element method calculations of hydrodynamic interactions between particles in close proximity. *Int. J. Numer. Meth. Fluids* 14 (1992) 1063-1086.

[9] M. G. Duffy, Quadrature over a pyramid or cube of integrands with a singularity at a vertex. *SIAM J. Numer. Anal*. 19 (1982), 1260-1262.

[10] R. Cortez, The method of regularized Stokeslets. *SIAM J. Sci. Comput*. 23 (2001) 1204-1225.

[11] H. Takahasi and M. Mori, Double exponential formulas for numerical integration. Publications of RIMS 9 (1974), 721-741.

[12] N. Max, Weights for computing vertex normals from facet normals. *Journal of Graphics Tools* 4 (1999), 1-6.

[13] S. Jin, R. R. Lewis and D. West, A comparison of algorithms for vertex normal computation. *The Visual Computer*.

[14] D. H. Bailey, Tanh-Sinh High-Precision Quadrature. Available at http://crd.lbl.gov/~dhbailey/dhbpapers/dhb-tanh-sinh.pdf.

[15] L. Ye, Numerical Quadrature: Theory and Computation. Master Thesis, Dalhousie University, Halifax, Nova Scotia, (2006).

[16] H. Zhao, A. H. G. Isfahani, L. N. Olson, and J. B. Freund, A spectral boundary integral method for flowing blood cells. *J. Comput. Phys*. 229 (2010), 3726-3744.